

Cloud-Resolving Modeling of Convective Processes

Shouting Gao · Xiaofan Li

Cloud-Resolving Modeling of Convective Processes

 Springer

Shouting Gao
Institute of Atmospheric Physics
Chinese Academy of Sciences
China

Xiaofan Li
NOAA/NESDIS Center for Satellite
Applications and Research
MD, USA

ISBN 978-1-4020-8275-7

e-ISBN 978-1-4020-8276-4

Library of Congress Control Number: 2008923288

All Rights Reserved

© 2008 Springer Science+Business Media B.V.

No part of this work may be reproduced, stored in a retrieval system, or transmitted in any form or by any means, electronic, mechanical, photocopying, microfilming, recording or otherwise, without written permission from the Publisher, with the exception of any material supplied specifically for the purpose of being entered and executed on a computer system, for exclusive use by the purchaser of the work.

Printed on acid-free paper

9 8 7 6 5 4 3 2 1

springer.com

Foreword

Clouds and cloud systems and their interactions with larger scales of motion, radiation, and the Earth's surface are extremely important parts of weather and climate systems. Their treatment in weather forecast and climate models is a significant source of errors and uncertainty. As computer power increases, it is beginning to be possible to explicitly resolve cloud and precipitation processes in these models, presenting opportunities for improving precipitation forecasts and larger-scale phenomena such as tropical cyclones which depend critically on cloud and precipitation physics.

This book by Professor Shouting Gao of the Institute of Atmospheric Physics in Beijing and Dr. Xiaofan Li of NOAA's National Environmental Satellite, Data, and Information Service (NESDIS) presents an update and review of results of high-resolution, mostly two-dimensional models of clouds and precipitation and their interactions with larger scales of motion and the Earth's surface. It provides a thorough description of cloud and precipitation physics, including basic governing equations and related physics, such as phase changes of water, radiation, and mixing. Model results are compared with observations from the 1992–93 Tropical Ocean Global Atmosphere Coupled Ocean Atmosphere Response Experiment (TOGA COARE) experiment. The importance of the ocean to tropical convective systems is clearly shown here in the numerical results of simulations with their air–sea coupled modeling system. While the focus is on tropical convection, the methodology and applicability can be extended to cloud and precipitation processes elsewhere.

The results described in this well-written book form a solid foundation for future high-resolution model weather forecasts and climate simulations that resolve clouds explicitly in three dimensions – a future that I believe has great promise for the understanding and prediction of weather and climate for the great benefit of society.

University Corporation for Atmospheric Research,
June 2007

Richard Anthes
President

Contents

Foreword	v
Introduction	xi
1 Model and Physics	1
1.1 Governing Equations	1
1.2 Cloud Microphysical Parameterization Schemes	9
1.3 Radiation Parameterization Schemes	14
1.4 Subgrid-Scale Turbulence Closure	16
1.5 Boundary Conditions and Basic Parameters	17
References	18
2 Analysis Methodology	23
2.1 Heat and Vapor Budgets	23
2.2 Surface Rainfall Equation	24
2.3 Energetics Equations in Moist Atmosphere and Convective Available Potential Energy	25
2.4 Ocean Mixed-Layer Thermal and Saline Budgets	29
2.5 Partition of Convective and Stratiform Clouds	30
References	32
3 Comparison Between Simulations and Observations	35
3.1 Comparison Between Simulations and Observations	35
3.2 Model Responses to Initial Moisture Perturbations	41
3.3 Comparison Between 2D and 3D Simulations	51
References	52
4 Surface Rainfall Processes	55
4.1 Time Series of Zonal-Mean Surface Rain Rate	56
4.2 Time-Mean Surface Rainfall Processes	60
4.3 Surface Rainfall Processes Associated with Individual Cloud	62
References	64

5	Tropical Cloud Clusters	65
5.1	Introduction	65
5.2	Kinetics and Spatial Structures of Cloud Clusters	66
5.3	Cloud Merger	67
5.4	Surface Rainfall Processes Associated with Cloud Clusters	71
	References	73
6	Cloud Radiative and Microphysical Processes	75
6.1	Radiative Processes	75
6.2	Cloud Microphysical Processes	78
6.3	Impacts of Ice Microphysics in Development of Tropical Convection	81
6.4	Interaction Between Water and Ice Clouds	86
6.5	Condensation, Associated Heating, and Large-Scale Forcing	94
6.6	Phase Relation Between Unstable Energy and Surface Rainfall	100
	References	101
7	Convective, Moist, and Dynamic Vorticity Vectors	105
7.1	Convective Vorticity Vector	105
7.2	Moist Vorticity Vector	111
7.3	Dynamic Vorticity Vector	115
	References	118
8	Diurnal Variations of Tropical Oceanic Convection	121
8.1	Introduction	121
8.2	Diurnal Variation of Zonal-Mean Surface Rainfall	123
8.3	Diurnal Analysis with Grid Simulation Data from a Coupled Model	127
8.4	Diurnal Variations of Convective and Stratiform Rainfall	130
	References	135
9	Precipitation Efficiency	137
	References	146
10	Air–Sea Coupling	147
10.1	Introduction	147
10.2	Development of a Cloud-Resolving Air–Sea Coupling System	148
10.3	Role of Air–Sea Coupling in Surface Rainfall Process	152
	References	154
11	Climate Equilibrium States	157
11.1	Introduction	157
11.2	Effects of <i>SST</i> on Equilibrium Climate	160
11.3	Effects of Diurnal Variation on Equilibrium Climate	165
11.4	Cloud Microphysical and Radiative Effects on Equilibrium Climate	172
11.5	Effects of Zonal Perturbations of <i>SST</i> on Equilibrium States	179
	References	183

12 Remote Sensing Applications 185

 12.1 Introduction 185

 12.2 AMSU Responses to Cloud Hydrometeors 187

 12.3 Correction of Cloud Contamination on AMSU Measurements 191

 12.4 Comparison Studies Between Simulated and Observed Radiances .. 192

 References 196

13 Future Perspective of Cloud-Resolving Modeling 199

 13.1 Simplification of Cloud Microphysical Parameterization Schemes .. 199

 13.2 Cloud-Resolving Convection Parameterization 201

 13.3 Global Cloud-Resolving Model 203

 References 204

Abbreviations and Acronyms 205

Index 207

Introduction

The material in this book is based on our recent research work in the last 10 years. This is the first book that focuses on cloud-resolving modeling of convective processes. Clouds play an important role in linking atmospheric and hydrological processes and have profound impacts on regional and global climate. Better description of clouds and associated cloud–radiation interaction is a key for successful simulations of cloud processes, which requires the physical presence of cloud hydrometeors, prognostic cloud equations, and interactive radiative schemes in models. Cloud-resolving models have been developing for four decades towards providing better understanding of cloud-scale processes associated with convective development. With the explosive increase of computational powers, the cloud-resolving models which were once used to develop cloud schemes for general circulation models have been directly applied to a global domain with a high horizontal resolution (grid mesh is less than 5 km), whose preliminary results are promising.

This book starts with basic equations and physical packages used in cloud-resolving models and coupled ocean-cloud-resolving atmosphere model. The cloud-resolving model discussed in this book is the two-dimensional version of the Goddard Cumulus Ensemble Model. The model simulations are evaluated with available observations during Tropical Ocean Global Atmosphere Coupled Ocean-Atmosphere Response Experiment (TOGA COARE). The book covers many research aspects related to convective development, cloud, and precipitation. The material in this book has been used as part of a graduate course at the Graduate School, Chinese Academy of Sciences, Beijing, China. Therefore, this book can be used as a reference and textbook for graduate students and researchers whose research interests are mesoscale, cloud, and precipitation modeling.

This book is comprised of 13 chapters. Chapter 1 presents governing equations, parameterization schemes of radiation, cloud microphysics, and subgrid-scale turbulence. Two model frameworks imposed by different large-scale forcing are intensively discussed. Chapter 2 describes thermal and vapor budgets, surface rainfall equation, energetics equation, and partitioning of convective and stratiform rainfall, which are frequently applied to the analysis of cloud-resolving model simulation

data. The cloud-resolving model simulation data are evaluated with the high-quality observational data from TOGA COARE in terms of thermodynamic states, apparent heat sink and moisture source, surface radiative and latent heat fluxes, and surface rain rate in chapter 3. Since most of the research work is from two-dimensional cloud-resolving modeling, the similarities and differences between two- and three-dimensional cloud-resolving modeling are discussed.

The surface rainfall equation is introduced to examine the contributions of water vapor and cloud hydrometeors in surface rainfall processes in chapter 4. The intensive discussions of surface rainfall processes are conducted in raining stratiform, convective, nonraining stratiform, and clear-sky regions, respectively. In chapter 5, kinematics and propagation of tropical cloud clusters are discussed. Chapter 6 addresses cloud microphysics and radiation. In particular, the depositional growth of snow from cloud ice as an important sink of cloud ice, and precipitation–radiation interaction are interactively examined. The vorticity vectors associated with tropical convection are discussed in chapter 7. The dominant physical processes that are responsible for the diurnal variations of tropical convection including nocturnal and afternoon rainfall peaks and tropical convective and stratiform rainfall are quantitatively identified with analysis of surface rainfall equation in chapter 8. The precipitation efficiencies and statistical equivalence of efficiencies defined with water vapor and cloud-microphysics budgets are addressed in chapter 9. The coupled ocean-cloud-resolving atmosphere model is developed to study the small-scale effects of precipitation in ocean mixing processes in chapter 10. Effects of SST, diurnal variation, and cloud radiation on equilibrium states are discussed in chapter 11. The microwave radiative transfer model with cloud-resolving model simulation data is applied to radiance simulations in chapter 12. Finally, the future perspective of cloud-resolving modeling including simplification of prognostic cloud schemes, application of cloud-resolving modeling to general circulation model and to global domain are discussed in chapter 13.

We would like to thank Dr. Richard A. Anthes, President of the University Corporation for Atmospheric Research, who read the book draft and wrote the preface for this book. Our sincere thanks also go to Dr. Wei-Kuo Tao and Dr. David Adamec at NASA/Goddard Space Flight Center (GSFC), Professor Ming-Dah Chou at National Taiwan University, and Professor Minghua Zhang at the State University of New York, Stony Brook for providing two-dimensional Goddard Cumulus Ensemble (GCE) model, ocean mixed-layer model, radiative transfer code used in GCE model, and TOGA COARE forcing data, respectively. We also thank Dr. Hsiao-Ming Hsu at the National Center for Atmospheric Research for his comments, Drs. Fan Ping, Xiaopeng Cui, Yushu Zhou, and Lingkun Ran at the Institute of Atmospheric Physics, Chinese Academy of Sciences, for efficient and productive research collaborations, and Miss Di Li at the University of Maryland, College Park, for editing this book. Xiaofan Li would like to thank Dr. William K.-M. Lau, Chief of the Laboratory for Atmospheres at NASA/GSFC, and Professor Chung-Hsiung Sui at the National Central University for their support, encouragement, and academic guidance when Xiaofan Li worked at GSFC as a contract research scientist during 1994–2001, Drs. Fuzhong Weng and Quanhua Liu at NOAA/NESDIS/Center

for Satellite Applications and Research for providing microwave radiative transfer model, and Dr. Jian-Jian Wang at the Goddard Center for Earth Science and Technology, University of Maryland, Baltimore County, for research collaboration.

We are also indebted to Dr. Robert Doe and Ms. Nina Bennink at Springer for their editorial efforts. This work was supported by the national Key Basic Research and Development Projects of China under the grants No. 2004CB418301 and G1998040907 and Olympic Meteorological Service Projects under grants No. 2001BA904B09 and KACX1-02.

Beijing, China
Camp Springs, Maryland, USA
Fall 2007

Shouting Gao
Xiaofan Li

Chapter 1

Model and Physics

Cloud-resolving models differ from general circulation and mesoscale models in two ways. First, they cannot simulate large-scale circulations due to small model domains, whereas general circulation and mesoscale models can simulate large-scale circulations. A large-scale forcing is imposed in the cloud-resolving model. Second, cloud-resolving models with fine spatial resolutions use prognostic cloud microphysical parameterization to simulate cloud and precipitation processes. In contrast, general circulation and mesoscale models use diagnostic cumulus parameterization and/or prognostic cloud microphysical parameterization due to coarse spatial resolutions. Many cloud-resolving models have been developed to study convective responses to the large-scale forcing (Table 1.1). In this chapter, the cloud-resolving model and coupled ocean-cloud-resolving atmosphere model will be described in a two-dimensional (2D) framework in terms of governing equations, large-scale forcing, parameterization schemes of cloud microphysics, radiation, subgrid-scale turbulence closure, ocean mixing closure, and boundary conditions.

1.1 Governing Equations

The cloud-resolving model was originally developed by Soong and Ogura (1980) and Soong and Tao (1980). This model was significantly improved by Tao and Simpson (1993) at the National Aeronautics and Space Administration (NASA) Goddard Space Flight Center (GSFC) and was modified by Sui et al. (1994, 1998). The model was named the Goddard cumulus ensemble (GCE) model. The cloud-resolving model used in this book is the 2D-modified version of GCE model. The nonhydrostatic governing equations with an elastic approximation can be expressed by

$$\nabla \cdot \mathbf{V} + \frac{1}{\bar{\rho}} \frac{\partial}{\partial z} \bar{\rho} w = 0, \quad (1.1a)$$

$$\frac{\partial A}{\partial t} = -\nabla \cdot \mathbf{V} A - \frac{1}{\bar{\rho}} \frac{\partial}{\partial z} \bar{\rho} w A + S_A + D_A, \quad (1.1b)$$

$$\frac{\partial B}{\partial t} = -\nabla \cdot \mathbf{V} B - \frac{1}{\bar{\rho}} \frac{\partial}{\partial z} \bar{\rho} (w - w_{TB}) B + S_B + D_B. \quad (1.1c)$$

Table 1.1 A summary of cloud-resolving models

Model	Dynamic core	Cloud scheme	Turbulence closures	Radiation scheme
Clark (1977, 1979), Clark and Hall (1991), Clark et al. (1996)	Anelastic and hydrostatic approximations	Water cloud (Kessler 1969), ice cloud (Koenig and Murray 1976)	Smagorinsky (1963), Lilly (1962)	Kiehl et al. (1994)
Soong and Ogura (1980), Tao and Simpson (1993)	Anelastic approximation and nonhydrostatic form	Water and ice schemes (Lin et al. 1983, Rutledge and Hobbs 1983, 1984; Tao et al. 1989; Krueger et al. 1995)	Klemp and Wilhelmson (1978)	Solar (Chou et al. 1998) and IR infrared (Chou et al. 1991; Chou and Suarez 1994) schemes
Lipps and Hemler (1986, 1988, 1991)	Anelastic and hydrostatic approximations	Water cloud (Kessler 1969)	Klemp and Wilhelmson (1978)	Newtonian damping
Redelsperger and Sommeria (1986)	Deardorff (1972), Sommeria (1976), Redelsperger and Sommeria (1981a, b, 1982)	Water cloud (Kessler 1969)	Subgrid-scale turbulence closure (Redelsperger and Sommeria (1981a, b, 1982)	–
Hu and He (1988), Hu et al. (1998), Zou (1991)	Nonhydrostatic primitive dynamic core (Zou 1991)	Prognostic equations for hydrometeors and number concentrations (Hu and He 1988)	Second-moment turbulence closure	–
Krueger (1988)	Anelastic and hydrostatic approximations	Three-phase bulk scheme (Lin et al. 1983; Lord et al. 1984; Krueger et al. 1995)	Third-moment turbulence closure (Krueger 1988)	Harshvardhan et al. (1987)
Nakajima and Matsuno (1988)	Yamasaki (1975), Ogura and Philips (1962)	Water cloud (Kessler 1969)	Velocity deformation and static stability dependent	Horizontal homogeneous cooling

Tripoli (1992)	Nonhydrostatic core with enstrophy conservation	Flatau et al. (1989)	A turbulent kinetic closure for eddy diffusion	Chen and Cotton (1983)
Xu (1992), Xu and Huang (1994)	Nonhydrostatic primitive dynamic core	Xu and Duan (1999)	Second-moment turbulence closure	-
Ferrier (1994), Ferrier et al. (1995)	Anelastic approximation and nonhydrostatic form	Double-moment multiple-phase four-class ice scheme (Ferrier 1994)	Klemp and Wilhelmson (1978)	Chou (1984, 1986), Chou and Kouvaris (1991)
Tompkins and Craig (1998)	Anelastic quasi-Boussinesq approximation	Three-phase ice scheme (Swann 1994; Brown and Swann 1997); the water vapor and cloud water are combined into the total-water mixing ratio	First-order subgrid-scale turbulence closure (Shutts and Gray 1994)	Two-stream plane-parallel approximation (Edwards and Slingo 1996; Petch 1998)
Sato et al. (2005)	Nonhydrostatic formulations in the icosahedral grids covering the global domain	Grabowski (1998)	Mellor and Yamada (1974) level-2 closure	Nakajima et al. (2000)

Here, \mathbf{V} and w are horizontal wind vector and vertical wind, respectively; $\bar{\rho}$ is a mean density, which is a function of height only; $A = (\theta, q_v, \mathbf{V}, w)$; $B = (q_c, q_r, q_i, q_s, q_g)$; θ and q_v are potential temperature and specific humidity, respectively; q_c, q_r, q_i, q_s, q_g are the mixing ratios of cloud water (small cloud droplets), raindrops, cloud ice (small ice crystals), snow (density 0.1 g cm^{-3}), and graupel (density 0.4 g cm^{-3}), respectively; w_{TB} is a terminal velocity that is zero for cloud water and ice; S_A is a source and sink in momentum, temperature, and moisture equations such as pressure gradient force, buoyancy force, condensational heating, and radiative heating. The radiation parameterization schemes will be addressed in section 1.3; S_B is a cloud source and sink that is determined by microphysical processes, which will be discussed in section 1.2; D_A and D_B are dissipation terms related to subgrid-scale turbulence closure, which will be elucidated in section 1.4.

For model calculations by Li et al. (1999), it is convenient to partition (A, \mathbf{V}) into area means $(\bar{A}, \bar{\mathbf{V}})$ and deviations (A', \mathbf{V}') , i.e.,

$$A = \bar{A} + A', \quad (1.2a)$$

$$\mathbf{V} = \bar{\mathbf{V}} + \mathbf{V}'. \quad (1.2b)$$

Applying (1.2) to (1.1b) leads to

$$\begin{aligned} \frac{\partial A}{\partial t} = & -\nabla \cdot (\mathbf{V}'A' + \mathbf{V}'\bar{A} + \bar{\mathbf{V}}A') - \frac{1}{\bar{\rho}} \frac{\partial}{\partial z} \bar{\rho} (w'A' + w'\bar{A} + \bar{w}A') \\ & + S_A + D_A - \bar{\mathbf{V}} \cdot \nabla \bar{A} - \bar{w} \frac{\partial}{\partial z} \bar{A}. \end{aligned} \quad (1.3)$$

Here, the area mean continuity equation (1.1a) is used in the derivation of (1.3).

Taking an area mean over (1.3), we get the equation for \bar{A} ,

$$\frac{\partial \bar{A}}{\partial t} = -\nabla \cdot \overline{\mathbf{V}'A'} - \frac{1}{\bar{\rho}} \frac{\partial}{\partial z} \bar{\rho} \overline{w'A'} + \bar{S}_A + \bar{D}_A - \bar{\mathbf{V}} \cdot \nabla \bar{A} - \bar{w} \frac{\partial}{\partial z} \bar{A}. \quad (1.4a)$$

Perturbation equation for A' is obtained by subtracting (1.4a) from (1.3):

$$\begin{aligned} \frac{\partial A'}{\partial t} = & -\nabla \cdot (\mathbf{V}'\bar{A} + \bar{\mathbf{V}}A') - \frac{1}{\bar{\rho}} \frac{\partial}{\partial z} \bar{\rho} (w'\bar{A} + \bar{w}A') - \nabla \cdot (\mathbf{V}'A' - \overline{\mathbf{V}'A'}) \\ & - \frac{1}{\bar{\rho}} \frac{\partial}{\partial z} \bar{\rho} (w'A' - \overline{w'A'}) + S_A - \bar{S}_A + D_A - \bar{D}_A. \end{aligned} \quad (1.4b)$$

Environment has an important impact on convective development. When convection develops, associated momentum, heat, and moisture transport upward through convective activity, which in turn modify environment significantly. Environment and convection interact in a nonlinear way (e.g., Chao 1962). Due to a small domain in the cloud-resolving model (e.g., 768 km in a 2D framework), the large-scale circulation cannot be simulated. Thus, the large-scale forcing needs to be imposed in the cloud-resolving model. Soong and Ogura (1980) were the first to develop ways to impose the observed large-scale variables into the cloud-resolving model

to examine the convective response to the imposed large-scale forcing. The major forcing is vertical velocity and associated vertical advections. Thus, there are two ways to impose the large-scale forcing into the cloud model. The horizontally uniform and vertically varying vertical velocity can be imposed, as first introduced by Soong and Ogura (1980), or the horizontally uniform total advection of the heat and moisture can be imposed (e.g., Wu et al. 1998). Li et al. (1999) discussed the two model setups intensively.

For the model with the imposed vertical velocity (\bar{w}^o), horizontal wind ($\bar{\mathbf{V}}^o$) and horizontal advection ($-\bar{\mathbf{V}}^o \cdot \nabla \bar{A}^o$) are also imposed. These forcing data denoted by superscript “ o ” are calculated from the observational data [e.g., Tropical Ocean Global Atmosphere Coupled Ocean-Atmosphere Response Experiment (TOGA COARE) in Li et al. (1999) and Global Atmosphere Research Program (GARP) Atlantic Tropical Experiment (GATE) in Grabowski et al. (1996)]. With the assumption that $-\mathbf{V}' \cdot \nabla \bar{A}^o = 0$, the model equations for potential temperature and specific humidity can be expressed by

$$\begin{aligned} \frac{\partial A}{\partial t} = & -\nabla \cdot \mathbf{V}' A' - \bar{\mathbf{V}}^o \cdot \nabla A' - \frac{1}{\bar{\rho}} \frac{\partial}{\partial z} \bar{\rho} w' A' - \bar{w}^o \frac{\partial}{\partial z} A' - w' \frac{\partial}{\partial z} \bar{A} \\ & + S_A + D_A - \bar{\mathbf{V}}^o \cdot \nabla \bar{A}^o - \bar{w}^o \frac{\partial}{\partial z} \bar{A}. \end{aligned} \quad (1.5)$$

The model consists of (1.1a) and (1.1c), perturbation momentum equation (1.4b), and equations for potential temperature and specific humidity (1.5).

For the model with imposed horizontally uniform total advection of heat and moisture, horizontal wind is also imposed. With the assumption that $-\nabla \cdot \bar{\mathbf{V}}^o A' - \partial \bar{\rho} A' \bar{w}^o / \bar{\rho} \partial z = 0$, the model equations for potential temperature and specific humidity can be written by

$$\frac{\partial A}{\partial t} = -\nabla \cdot \mathbf{V}' A - \frac{1}{\bar{\rho}} \frac{\partial}{\partial z} \bar{\rho} w' A + S_A + D_A - \bar{\mathbf{V}}^o \cdot \nabla \bar{A}^o - \bar{w}^o \frac{\partial}{\partial z} \bar{A}^o \quad (1.6)$$

This model is comprised of (1.1a) and (1.1c), perturbation momentum equation (1.4b), and equations for potential temperature and specific humidity (1.6). Li et al. (1999) found that the terms omitted in (1.5) and (1.6) do not have any impact on the model simulations. The comparison between simulations by the two model setups will be discussed with the TOGA COARE data in chapter 3.

The governing equations in the 2D cloud-resolving model can be expressed as follows:

$$\frac{\partial u'}{\partial x} + \frac{1}{\bar{\rho}} \frac{\partial (\bar{\rho} w')}{\partial z} = 0, \quad (1.7a)$$

$$\begin{aligned} \frac{\partial u'}{\partial t} = & -\frac{\partial}{\partial x} (2u' \bar{u}^o + u' u') - \frac{1}{\bar{\rho}} \frac{\partial}{\partial z} \bar{\rho} (w' \bar{u}^o + \bar{w}^o u' + w' u' - \overline{w' u'}) \\ & - c_p \frac{\partial (\bar{\theta} \pi')}{\partial x} + D_u - \bar{D}_u, \end{aligned} \quad (1.7b)$$

$$\begin{aligned} \frac{\partial w'}{\partial t} = & -\frac{\partial}{\partial x}(u'\bar{w}^o + \bar{u}^o w' + u'w') - \frac{1}{\bar{\rho}} \frac{\partial}{\partial z} \bar{\rho}(2w'\bar{w}^o + w'w' - \overline{w'w'}) \\ & - c_p \frac{\partial(\bar{\theta}\pi')}{\partial z} + g \left(\frac{\theta'}{\theta_o} + 0.61q_v' - q_l' \right) + D_w - \bar{D}_w \end{aligned} \quad (1.7c)$$

$$\begin{aligned} \frac{\partial \theta}{\partial t} = & -\frac{\partial(u'\theta')}{\partial x} - \bar{u}^o \frac{\partial \theta'}{\partial x} - \frac{1}{\bar{\rho}} \frac{\partial}{\partial z} (\bar{\rho}w'\theta') - \bar{w}^o \frac{\partial \theta'}{\partial z} - w' \frac{\partial \bar{\theta}}{\partial z} \\ & + \frac{Q_{cn}}{\pi c_p} + \frac{Q_R}{\pi c_p} - \bar{u}^o \frac{\partial \bar{\theta}^o}{\partial x} - \bar{w}^o \frac{\partial \bar{\theta}}{\partial z} + D_\theta \end{aligned} \quad (1.7d)$$

$$\begin{aligned} \frac{\partial q_v}{\partial t} = & -\frac{\partial(u'q_v')}{\partial x} - \bar{u}^o \frac{\partial q_v'}{\partial x} - \bar{w}^o \frac{\partial q_v'}{\partial z} - w' \frac{\partial \bar{q}_v}{\partial z} - \frac{1}{\bar{\rho}} \frac{\partial}{\partial z} \bar{\rho}w'q_v' \\ & - S_{qv} - \bar{u}^o \frac{\partial \bar{q}_v^o}{\partial x} - \bar{w}^o \frac{\partial \bar{q}_v}{\partial z} + D_{qv} \end{aligned} \quad (1.7e)$$

$$\frac{\partial q_c}{\partial t} = -\frac{\partial(uq_c)}{\partial x} - \frac{1}{\bar{\rho}} \frac{\partial(\bar{\rho}wq_c)}{\partial z} + S_{qc} + D_{qc}, \quad (1.7f)$$

$$\frac{\partial q_r}{\partial t} = -\frac{\partial(uq_r)}{\partial x} - \frac{1}{\bar{\rho}} \frac{\partial}{\partial z} \bar{\rho}(w - w_{Tr})q_r + S_{qr} + D_{qr}, \quad (1.7g)$$

$$\frac{\partial q_i}{\partial t} = -\frac{\partial(uq_i)}{\partial x} - \frac{1}{\bar{\rho}} \frac{\partial(\bar{\rho}wq_i)}{\partial z} + S_{qi} + D_{qi}, \quad (1.7h)$$

$$\frac{\partial q_s}{\partial t} = -\frac{\partial(uq_s)}{\partial x} - \frac{1}{\bar{\rho}} \frac{\partial}{\partial z} \bar{\rho}(w - w_{Ts})q_s + S_{qs} + D_{qs}, \quad (1.7i)$$

$$\frac{\partial q_g}{\partial t} = -\frac{\partial(uq_g)}{\partial x} - \frac{1}{\bar{\rho}} \frac{\partial}{\partial z} \bar{\rho}(w - w_{Tg})q_g + S_{qg} + D_{qg}, \quad (1.7j)$$

where

$$\begin{aligned} Q_{cn} = & L_v(PCND - P_{REVP}) + L_s \{ P_{DEP} + (1 - \delta_1)P_{SDEP}(T < T_o) \\ & + (1 - \delta_1)P_{GDEP}(T < T_o) - P_{MLTS}(T > T_o) \\ & - P_{MLTG}(T > T_o) \} \\ & + L_f \{ P_{SACW}(T < T_o) + P_{SFW}(T < T_o) + P_{GACW}(T < T_o) \\ & + P_{IACR}(T < T_o) + P_{GACR}(T < T_o) + P_{SACR}(T < T_o) \\ & + P_{GFR}(T < T_o) - P_{RACS}(T > T_o) - P_{SMLT}(T > T_o) \\ & - P_{GMLT}(T > T_o) + P_{IHOM}(T < T_{oo}) \\ & - P_{IMLT}(T > T_o) + P_{IDW}(T_{oo} < T < T_o) \}, \end{aligned} \quad (1.8a)$$

$$S_{qv} = PCND - P_{REVP} + P_{DEP} + (1 - \delta_1)P_{SDEP}(T < T_o) + (1 - \delta_1)P_{GDEP}(T < T_o) - P_{MLTS}(T > T_o) - P_{MLTG}(T > T_o), \quad (1.8b)$$

$$S_{qc} = -P_{SACW} - P_{RAUT} - P_{RACW} - P_{SFW}(T < T_o) - P_{GACW} + PCND - P_{IHOM}(T < T_{oo}) + P_{IMLT}(T > T_o) - P_{IDW}(T_{oo} < T < T_o), \quad (1.8c)$$

$$\begin{aligned}
S_{qr} = & P_{SACW}(T > T_o) + P_{RAUT} + P_{RACW} + P_{GACW}(T > T_o) \\
& - P_{REVP} + P_{RACS}(T > T_o) - P_{IACR}(T < T_o) - P_{GACR}(T < T_o) \\
& - P_{SACR}(T < T_o) - P_{GFR}(T < T_o) + P_{SMLT}(T > T_o) + P_{GMLT}(T > T_o),
\end{aligned} \tag{1.8d}$$

$$\begin{aligned}
S_{qi} = & -P_{SAUT}(T < T_o) - P_{SACI}(T < T_o) - P_{RACI}(T < T_o) \\
& - P_{SFI}(T < T_o) - P_{GACI}(T < T_o) + P_{IHOM}(T < T_{oo}) \\
& - P_{IMLT}(T > T_o) + P_{IDW}(T_{oo} < T < T_o) + P_{DEP},
\end{aligned} \tag{1.8e}$$

$$\begin{aligned}
S_{qs} = & P_{SAUT}(T < T_o) + P_{SACI}(T < T_o) + \delta_4 P_{SACW}(T < T_o) \\
& + P_{SFW}(T < T_o) + P_{SFI}(T < T_o) + \delta_3 P_{RACI}(T < T_o) \\
& - P_{RACS}(T > T_o) - P_{GACS} - P_{SMLT}(T > T_o) \\
& - (1 - \delta_2) P_{RACS}(T < T_o) + \delta_2 P_{SACR}(T < T_o) \\
& + (1 - \delta_1) P_{SDEP}(T < T_o) - P_{MLTS}(T > T_o) \\
& + \delta_3 P_{IACR}(T < T_o) - (1 - \delta_4) P_{WACS}(T < T_o),
\end{aligned} \tag{1.8f}$$

$$\begin{aligned}
S_{qg} = & + (1 - \delta_3) P_{RACI}(T < T_o) + P_{GACI}(T < T_o) \\
& + P_{GACW}(T < T_o) + (1 - \delta_4) P_{SACW}(T < T_o) + P_{GACS} \\
& + (1 - \delta_3) P_{IACR}(T < T_o) + P_{GACR}(T < T_o) \\
& + (1 - \delta_2) P_{RACS}(T < T_o) + P_{GFR}(T < T_o) \\
& + (1 - \delta_4) P_{WACS}(T < T_o) - P_{GMLT}(T > T_o) \\
& + (1 - \delta_1) P_{GDEP}(T < T_o) - P_{MLTG}(T > T_o) \\
& + (1 - \delta_2) P_{SACR}(T < T_o),
\end{aligned} \tag{1.8g}$$

and

$$\delta_1 = 1, \text{ only if } q_c + q_i > 10^{-8} \text{ gg}^{-1}, T < T_o, \tag{1.8h}$$

$$\delta_2 = 1, \text{ only if } q_s + q_r < 10^{-4} \text{ gg}^{-1}, T < T_o, \tag{1.8i}$$

$$\delta_3 = 1, \text{ only if } q_r > 10^{-4} \text{ gg}^{-1}, T < T_o, \tag{1.8j}$$

$$\delta_4 = 1, \text{ only if } q_s \leq 10^{-4} \text{ gg}^{-1}, q_c > 5 \times 10^{-4} \text{ gg}^{-1}, T < T_o. \tag{1.8k}$$

Here, $\pi = (p/p_o)^{\kappa}$, $\kappa = R/c_p$; R is the gas constant; c_p is the specific heat of dry air at constant pressure p , and $p_o = 1,000 \text{ mb}$; T is air temperature, and $T_o = 0^\circ\text{C}$, $T_{oo} = -35^\circ\text{C}$. L_v , L_s , and L_f are latent heat of vaporization, sublimation, and fusion at 0°C , respectively, and $L_s = L_v + L_f$. Q_R is the radiative heating rate due to convergence of the net flux of solar and infrared (IR) radiative fluxes, which will be discussed in section 1.3. The cloud microphysical terms in (1.8b–g) are defined in Table 1.2, which will be discussed in section 1.2. The cloud microphysical processes are also summarized in Fig. 1.1.

When the model is integrated over the ocean, a time-invariant or temporally varied horizontally uniform sea surface temperature (SST) is imposed in both model setups. Li et al. (2000) developed a coupled ocean-cloud-resolving atmosphere model to study the impacts of precipitation and associated salinity stratification in

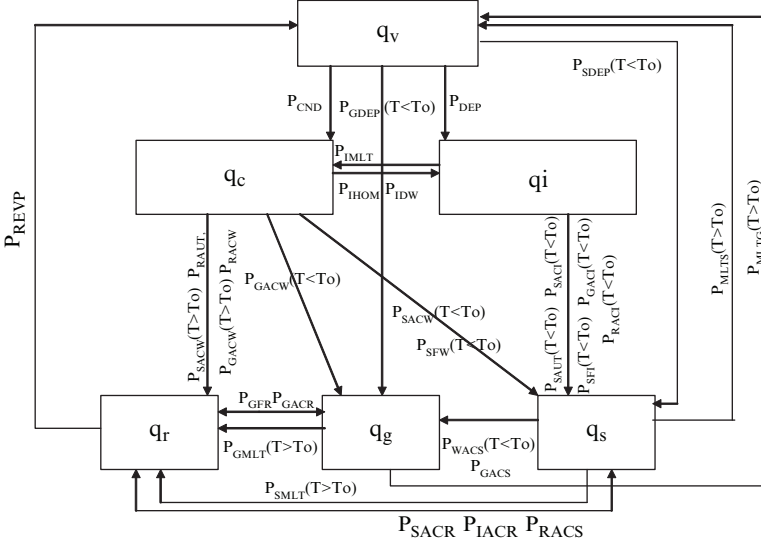


Fig. 1.1 A flowchart of the cloud microphysical schemes

ocean mixed-layer temperature and salinity at small spatial scales. An embedded mixed-layer ocean circulation model was originally developed by Adamec et al. (1981). The mixed-layer equations in the 2D framework are

$$\frac{\partial h_m}{\partial t} = -\frac{\partial u_m h_m}{\partial x} + W_e, \quad (1.9a)$$

$$\frac{\partial u_m}{\partial t} = -\frac{W_e}{h_m} H(W_e)(u_m - u_e) - \frac{\tau_o}{\rho_r h_m}, \quad (1.9b)$$

$$\frac{\partial T_m}{\partial t} = -\frac{W_e}{h_m} H(W_e)(T_m - T_e) - \frac{Q_o + I(0) - I(h_m)}{\rho_r c_w h_m}, \quad (1.9c)$$

$$\frac{\partial S_m}{\partial t} = -\frac{W_e}{h_m} H(W_e)(S_m - S_e) - \frac{S_m(P_s - E_s)}{\rho_r c_w h_m}. \quad (1.9d)$$

Here, T_m , S_m , u_m , and h_m are ocean mixed-layer temperature, salinity, zonal current, and depth respectively; T_e and S_e are temperature and salinity of the level just beneath the mixed layer, respectively; H is the Heavyside step function in which $H = 1$ as $W_e > 0$, while $H = 0$ as $W_e < 0$; ρ_r is a constant reference seawater density; c_w is the heat capacity of water; $I = I_o[re^{-\gamma_1 z} + (1-r)e^{-\gamma_2 z}]$, I_o is solar radiation at the ocean surface; γ_1 , γ_2 are attenuation parameters for solar radiation penetration, and z is positive downward with $z = 0$ being the ocean surface; Q_o is the sum of longwave radiation, sensible and latent heat at the ocean surface; P_s and E_s denote the rates of precipitation and evaporation at the ocean surface, respectively; W_e is the entrainment velocity at the mixed-layer base, which can be obtained by calculating Kraus–Turner’s equation that was originally derived by Niiler and Kraus (1977), modified by Sui et al. (1997), and is similar to Garper (1988),

$$\begin{aligned}
& W_e H(W_e) h_m g [\alpha(T_m - T_e) - \beta(S_m - S_e)] \\
& = 2m_s u_*^3 - \frac{h_m}{2} [(1 + m_b)B_o + (1 - m_b)|B_o|]
\end{aligned} \tag{1.10}$$

$$\begin{aligned}
B_o = \frac{g\alpha}{\rho_r c_w} \left\{ Q_o + \left[1 + r e^{-\gamma_1 h_m} + (1 - r) e^{-\gamma_2 h_m} - \frac{2r}{\gamma_1 h_m} (1 - e^{-\gamma_1 h_m}) \right. \right. \\
\left. \left. - \frac{2(1 - r)}{\gamma_2 h_m} (1 - e^{-\gamma_2 h_m}) \right] I_o \right\} + \frac{g}{\rho_r} \beta S_m (P_s - E_s),
\end{aligned} \tag{1.10a}$$

where u_* is a surface friction velocity; α and β describe the logarithmic expansion of ocean water density ρ_r as a function of temperature and salinity, respectively; g is the gravitational acceleration; m_s and m_b are turbulent mixing factors due to wind stirring and convection, respectively.

The 2D model equation for ocean circulations on the equator can be written as

$$\frac{\partial u_1}{\partial t} = -\frac{\partial u_1 u_1}{\partial x} - \frac{\partial w_1 u_1}{\partial z} + A_M \frac{\partial^2 u_1}{\partial x^2} + K_M \frac{\partial^2 u_1}{\partial z^2}, \tag{1.11a}$$

$$\frac{\partial T_1}{\partial t} = -\frac{\partial u_1 T_1}{\partial x} - \frac{\partial w_1 T_1}{\partial z} + A_T \frac{\partial^2 T_1}{\partial x^2} + K_T \frac{\partial^2 T_1}{\partial z^2} - \frac{1}{\rho_r c_w} \frac{\partial I}{\partial z}, \tag{1.11b}$$

$$\frac{\partial S_1}{\partial t} = -\frac{\partial u_1 S_1}{\partial x} - \frac{\partial w_1 S_1}{\partial z} + A_S \frac{\partial^2 S_1}{\partial x^2} + K_S \frac{\partial^2 S_1}{\partial z^2}, \tag{1.11c}$$

$$\frac{\partial u_1}{\partial x} + \frac{\partial w_1}{\partial z} = 0, \tag{1.11d}$$

$$\frac{\partial p_1}{\partial z} = -\rho_1 g, \tag{1.11e}$$

$$\rho_1 = \rho_r [1 - \alpha(T_1 - T_r) - \beta(S_1 - S_r)], \tag{1.11f}$$

where u_1 and w_1 are zonal and vertical components of ocean current, respectively; T_1 and S_1 are ocean temperature and salinity, respectively; A_M , A_T , and A_S are horizontal momentum, heat and salinity diffusivity coefficients, respectively; K_M , K_T , and K_S are vertical momentum, heat and salinity diffusivity coefficients, respectively; T_r and S_r are the reference temperature and salinity, respectively. The mixed-layer model and the ocean circulation model communicate with each other through the embedding technique proposed by Adamec et al. (1981). The model also includes a convective adjustment scheme that ensures the static stability of the upper ocean.

1.2 Cloud Microphysical Parameterization Schemes

The formulations of cloud microphysical parameterization schemes are documented in this section. Table 1.2 shows the list of microphysical processes and their parameterization schemes. The schemes are by Rutledge and Hobbs (1983, 1984), Lin et al. (1983), Tao et al. (1989), and Krueger et al. (1995).

Table 1.2 List of microphysical processes and their parameterization schemes. The schemes are Rutledge and Hobbs (1983, 1984; RH83, RH84), Lin et al. (1983, LFO), Tao et al. (1989, TSM), and Krueger et al. (1995, KFLC)

Notation	Description	Scheme
P_{MLTG}	Growth of vapor by evaporation of liquid from graupel surface	RH84
P_{MLTS}	Growth of vapor by evaporation of melting snow	RH83
P_{REVP}	Growth of vapor by evaporation of raindrops	RH83
P_{IMLT}	Growth of cloud water by melting of cloud ice	RH83
P_{CND}	Growth of cloud water by condensation of supersaturated vapor	TSM
P_{GMLT}	Growth of raindrops by melting of graupel	RH84
P_{SMLT}	Growth of raindrops by melting of snow	RH83
P_{RACI}	Growth of raindrops by the accretion of cloud ice	RH84
P_{RACW}	Growth of raindrops by the collection of cloud water	RH83
P_{RACS}	Growth of raindrops by the accretion of snow	RH84
P_{RAUT}	Growth of raindrops by the autoconversion of cloud water	LFO
P_{IDW}	Growth of cloud ice by the deposition of cloud water	KFLC
P_{IACR}	Growth of cloud ice by the accretion of rain	RH84
P_{IHOM}	Growth of cloud ice by the homogeneous freezing of cloud water	
P_{DEP}	Growth of cloud ice by the deposition of supersaturated vapor	TSM
P_{SAUT}	Growth of snow by the conversion of cloud ice	RH83
P_{SACI}	Growth of snow by the collection of cloud ice	RH83
P_{SACW}	Growth of snow by the accretion of cloud water	RH83
P_{SFW}	Growth of snow by the deposition of cloud water	KFLC
P_{SFI}	Depositional growth of snow from cloud ice	KFLC
P_{SACR}	Growth of snow by the accretion of raindrops	LFO
P_{SDEP}	Growth of snow by the deposition of vapor	RH83
P_{GACI}	Growth of graupel by the collection of cloud ice	RH84
P_{GACR}	Growth of graupel by the accretion of raindrops	RH84
P_{GACS}	Growth of graupel by the accretion of snow	RH84
P_{GACW}	Growth of graupel by the accretion of cloud water	RH84
P_{WACS}	Growth of graupel by the riming of snow	RH84
P_{GDEP}	Growth of graupel by the deposition of vapor	RH84
P_{GFR}	Growth of graupel by the freezing of raindrops	LFO

$$P_{MLTG} = \frac{2\pi N_{0G}(S-1)}{\rho(A'+B')} \left[\frac{0.78}{\lambda_G^2} + 0.31 \left(\frac{\bar{a}\rho}{\mu} \right)^{\frac{1}{2}} \left(\frac{\rho_o}{\rho} \right)^{\frac{1}{4}} \frac{\Gamma\left(\frac{\bar{b}+5}{2}\right)}{\lambda_G^{\frac{\bar{b}+5}{2}}} \right], \quad (1.12)$$

where $N_{0G}(=4 \times 10^6 \text{ m}^{-4})$ is the intercept value in graupel size distribution; $S(=q_w/q_{ws})$, where q_{ws} is the saturated mixing ratio with respect to water; $\bar{a}(=19.3 \text{ m}^{1-\bar{b}} \text{ s}^{-1})$ is the constant in fall-speed relation for graupel; $\bar{b}(=0.37)$ is the fall-speed exponent for graupel; $A' = L_v/K_a T (L_v M_w/RT - 1)$; $B' = RT/\chi M_w e_{ws}$ (Pruppacher and Klett (1978); $K_a(=2.43 \times 10^{-2} \text{ J m}^{-1} \text{ s}^{-1} \text{ K}^{-1})$ is the thermal conductivity coefficient of air; $M_w(=18.016)$ is the molecular weight of water; $\chi(=2.26 \times 10^{-5} \text{ m}^2 \text{ s}^{-1})$ is the diffusivity coefficient of water vapor in air; $R(=8.314 \times 10^3 \text{ J kmol}^{-1} \text{ K}^{-1})$ is the universal gas constant; e_{ws} is the saturation vapor pressure for water; $\lambda_G \left[= (\pi \rho_G N_{0G} / \rho q_g)^{\frac{1}{4}} \right]$ is the slope of graupel size distri-

bution; $\rho_G (=400 \text{ kg m}^{-3})$ is the density of graupel; $\mu (=1.718 \times 10^{-5} \text{ kg m}^{-1} \text{ s}^{-1})$ is the dynamic viscosity of air; Γ is the Gamma function.

$$P_{MLTS} = \frac{4N_{0S}(S-1)}{\rho(A'+B')} \left[\frac{0.65}{\lambda_S^2} + 0.44 \left(\frac{a''\rho}{\mu} \right)^2 \left(\frac{\rho_o}{\rho} \right)^{\frac{1}{4}} \frac{\Gamma\left(\frac{b+5}{2}\right)}{\lambda_S^{\frac{b+5}{2}}} \right], \quad (1.13)$$

where $N_{0S} (=4 \times 10^6 \text{ m}^{-4})$ is the intercept value in snowflake size distribution; $a'' (=1.139 \text{ m}^{1-b} \text{ s}^{-1})$ is the constant in fall-speed relation for snow; $b (=0.11)$ is the fall-speed exponent for snow; $\lambda_S [= (\pi\rho_S N_{0S} / \rho q_s)^{\frac{1}{4}}]$ is the slope of snowflake size distribution; $\rho_S (=100 \text{ kg m}^{-3})$ is the density of snow.

$$P_{REVP} = \frac{2\pi N_{0R}(S-1)}{\rho(A'+B')} \left[\frac{0.78}{\lambda_R^2} + 0.31 \left(\frac{a'\rho}{\mu} \right)^{\frac{1}{2}} \left(\frac{\rho_o}{\rho} \right)^{\frac{1}{4}} \frac{\Gamma(3)}{\lambda_R^3} \right], \quad (1.14)$$

where $N_{0R} (=8 \times 10^6 \text{ m}^{-4})$ is the intercept value in raindrop size distribution; $a' (=3 \times 10^3 \text{ s}^{-1})$ is the constant in linear fall-speed relation for raindrops; $\lambda_R [= (\pi\rho_L N_{0R} / \rho q_r)^{\frac{1}{4}}]$ is the slope of raindrop size distribution; $\rho_L (=10^3 \text{ kg m}^{-3})$ is the density of raindrops.

$$P_{IMLT} = \frac{q_i}{\Delta t}, \quad (1.15)$$

where Δt is the time step.

$$P_{CND} = \frac{1}{\Delta t} \frac{T - T_{oo}}{T_o - T_{oo}} \frac{q_v - (q_{qws} + q_{is})}{1 + \left(\frac{A_1 q_c q_{ws} + A_2 q_i q_{is}}{q_c + q_i} \right) \left(\frac{L_v(T - T_{oo}) + L_s(T_o - T)}{c_p(T_o - T_{oo})} \right)}, \quad (1.16)$$

where q_{is} is the saturation mixing ratio with respect to ice; $A_1 = 237.3B_1 / (T - 35.86)^2$; $A_2 = 265.5B_2 / (T - 7.66)^2$; $B_1 = 17.2693882$; $B_2 = 21.8745584$.

$$P_{GMLT} = -\frac{2\pi}{\rho L_f} K_a (T - T_o) N_{0G} \left[\frac{0.78}{\lambda_G^2} + 0.31 \left(\frac{\bar{a}\rho}{\mu} \right)^{\frac{1}{2}} \left(\frac{\rho_o}{\rho} \right)^{\frac{1}{4}} \frac{\Gamma\left(\frac{\bar{b}+5}{2}\right)}{\lambda_G^{\frac{\bar{b}+5}{2}}} \right], \quad (1.17)$$

$$P_{SMLT} = -\frac{2\pi}{\rho L_f} K_a (T - T_o) N_{0S} \left[\frac{0.65}{\lambda_S^2} + 0.44 \left(\frac{a''\rho}{\mu} \right)^{\frac{1}{2}} \left(\frac{\rho_o}{\rho} \right)^{\frac{1}{4}} \frac{\Gamma\left(\frac{b+5}{2}\right)}{\lambda_S^{\frac{b+5}{2}}} \right], \quad (1.18)$$

$$P_{RACI} = \frac{\pi}{4} q_i E_{RI} N_{0R} \left(\frac{\rho_o}{\rho} \right)^{\frac{1}{2}} \left[\frac{a_0 \Gamma(3)}{\lambda_R^3} + \frac{a_1 \Gamma(4)}{\lambda_R^4} + \frac{a_2 \Gamma(5)}{\lambda_R^5} + \frac{a_3 \Gamma(6)}{\lambda_R^6} \right], \quad (1.19)$$

where $E_{RI} (=1)$ is the rain/cloud ice collection efficiency coefficient; $a_0 = 0.267 \text{ m s}^{-1}$, $a_1 = 5.15 \times 10^3 \text{ s}^{-1}$, $a_2 = -1.0225 \times 10^6 \text{ m}^{-1} \text{ s}^{-1}$, $a_3 = 7.55 \times 10^7 \text{ m}^{-2} \text{ s}^{-1}$, which are the coefficients in polynomial fall-speed relation for raindrops.

$$P_{RACIW} = \frac{\pi}{4} q_c E_{RC} N_{0R} \left(\frac{\rho_o}{\rho} \right)^{\frac{1}{2}} \left[\frac{a_o \Gamma(3)}{\lambda_R^3} + \frac{a_1 \Gamma(4)}{\lambda_R^4} + \frac{a_2 \Gamma(5)}{\lambda_R^5} + \frac{a_3 \Gamma(6)}{\lambda_R^6} \right], \quad (1.20)$$

where $E_{RC}(=1)$ is the rain/cloud water collection efficiency coefficient.

$$P_{RACS} = E_{SR} \pi^2 \frac{\rho_s}{\rho} |\bar{V}_R - \bar{V}_S| N_{0R} N_{0S} \left(\frac{\rho_o}{\rho} \right)^{\frac{1}{2}} \left[\frac{5}{\lambda_S^6 \lambda_R} + \frac{2}{\lambda_S^5 \lambda_R^2} + \frac{1}{2 \lambda_S^4 \lambda_R^3} \right], \quad (1.21)$$

where $E_{SR}(=1)$ is the snow/rain collection efficiency coefficient;

$$\bar{V}_R = \left(-0.267 + \frac{206}{\lambda_R} - \frac{2.045 \times 10^3}{\lambda_R^2} + \frac{9.06 \times 10^3}{\lambda_R^3} \right) \left(\frac{\rho_o}{\rho} \right)^{\frac{1}{2}}, \quad (1.21a)$$

$$\bar{V}_S = a'' \frac{\Gamma(4+b)}{6 \lambda_S^b} \left(\frac{\rho_o}{\rho} \right)^{\frac{1}{2}}, \quad (1.21b)$$

where \bar{V}_R and \bar{V}_S are the mass-weighted fall-speed for rain and snow, respectively.

$$P_{RAUT} = \alpha (q_c - q_o), \quad (1.22)$$

where $\alpha(=10^{-3} \text{ s}^{-1})$ is the rate coefficient for auto-conversion; $q_o(=1.25 \times 10^{-3} \text{ g g}^{-1})$ is the mixing ratio threshold.

$$P_{IDW} = \frac{n_0 e^{\frac{1}{2}|T-T_o|}}{10^3 \rho} b_1 \left(\frac{\rho q_i}{n_0 e^{\frac{1}{2}|T-T_o|}} \right)^{b_2}, \quad (1.23)$$

where $n_0 = 10^{-8} \text{ m}^{-3}$; b_1 and b_2 are the positive temperature-dependent coefficients tabulated by Koenig (1971).

$$P_{IACR} = n_{ci} E_{RI} \frac{\pi^2}{24} \frac{\rho_L}{\rho} N_{0R} \left(\frac{\rho_o}{\rho} \right)^{\frac{1}{2}} \left[\frac{a_o \Gamma(6)}{\lambda_R^6} + \frac{a_1 \Gamma(7)}{\lambda_R^7} + \frac{a_2 \Gamma(8)}{\lambda_R^8} + \frac{a_3 \Gamma(9)}{\lambda_R^9} \right], \quad (1.24)$$

where $n_{ci}(= \rho q_i / \bar{M}_i)$ is the number concentration of cloud ice crystals; $\bar{M}_i(=6 \times 10^{-12} \text{ kg})$ is the average mass of a cloud ice particle.

$$P_{IHOM} = \frac{q_c}{\Delta t}, \quad (1.25)$$

$$P_{DEP} = \frac{1}{\Delta t} \frac{T_o - T}{T_o - T_{oo}} \frac{q_v - (q_{qws} + q_{is})}{1 + \left(\frac{A_1 q_c q_{ws} + A_2 q_i q_{is}}{q_c + q_i} \right) \left(\frac{L_v(T - T_{oo}) + L_s(T_o - T)}{c_p(T_o - T_{oo})} \right)}, \quad (1.26)$$

$$P_{SAUT} = \frac{\rho q_i - M_{\max} n_0 e^{0.6(T-T_o)}}{\rho \Delta t}, \quad (1.27)$$